EBioMedicine 18 (2017) 179–187

Contents lists available at ScienceDirect

EBioMedicine

journal homepage: www.ebiomedicine.com

Research Paper

Piperine Attenuates Pathological Cardiac Fibrosis Via PPAR-γ/AKT Pathways

Zhen-Guo Ma [a,b,c,1], Yu-Pei Yuan [a,b,c,1], Xin Zhang [a,b,c], Si-Chi Xu [a,b,c], Sha-Sha Wang [a,b,c], Qi-Zhu Tang [a,b,c,*]

[a] Department of Cardiology, Renmin Hospital of Wuhan University, Wuhan 430060, PR China
[b] Cardiovascular Research Institute of Wuhan University, Wuhan 430060, PR China
[c] Hubei Key Laboratory of Cardiology, Wuhan 430060, PR China

ARTICLE INFO

Article history:
Received 21 January 2017
Received in revised form 2 March 2017
Accepted 13 March 2017
Available online 14 March 2017

Keywords:
Piperine
Fibrosis
Cardiac fibroblast
PPAR-γ
AKT

ABSTRACT

Mitogen-activated protein kinases (MAPKs) and AMP-activated protein kinase α (AMPKα) play critical roles in the process of cardiac hypertrophy. Previous studies have demonstrated that piperine activates AMPKα and reduces the phosphorylation of extracellular signal-regulated kinase (ERK). However, the effect of piperine on cardiac hypertrophy remains completely unknown. Here, we show that piperine-treated mice had similar hypertrophic responses as mice treated with vehicle but exhibited significantly attenuated cardiac fibrosis after pressure overload or isoprenaline (ISO) injection. Piperine inhibited the transformation of cardiac fibroblasts to myofibroblasts induced by transforming growth factor-β (TGF-β) or angiotensin II (Ang II) in vitro. This anti-fibrotic effect was independent of the AMPKα and MAPK pathway. Piperine blocked activation of protein kinase B (AKT) and, downstream, glycogen synthase kinase 3β (GSK3β). The overexpression of constitutively active AKT or the knockdown of *GSK3β* completely abolished the piperine-mediated protection of cardiac fibroblasts. The cardioprotective effects of piperine were blocked in mice with constitutively active AKT. Pretreatment with GW9662, a specific inhibitor of peroxisome proliferator activated receptor-γ (PPAR-γ), reversed the effect elicited by piperine in vitro. In conclusion, piperine attenuated cardiac fibrosis via the activation of PPAR-γ and the resultant inhibition of AKT/GSK3β.

1. Introduction

Cardiac hypertrophy is an adaptive response to increased biomechanical loads and is characterized by myocyte hypertrophy, fibroblast activation, and extracellular matrix accumulation, ultimately leading to congestive heart failure and sudden death (Frey and Olson, 2003; Heineke and Molkentin, 2006). Increasing evidence suggests that mitogen-activated protein kinases (MAPKs) and AMP-activated protein kinase α (AMPKα) play critical roles in the process of pathological cardiac hypertrophy (Chan and Dyck, 2005; Lorenz et al., 2009; Ravingerova et al., 2003; Zhang et al., 2008). Therefore, pharmacological interventions in these signaling pathways could be of great therapeutic interest for treating cardiac hypertrophy.

In addition to cardiomyocytes, cardiac fibroblasts (CFs) are involved in orchestrating a pathological hypertrophic response (Kamo et al., 2015). The expression of transforming growth factor-β (TGF-β) was increased in the hypertrophied hearts induced by pressure overload (Dobaczewski et al., 2011). TGF-β directly induced the transformation of fibroblasts to myofibroblasts, which secrete hypertrophic and profibrotic factors and result in extracellular matrix protein deposition (Butt et al., 1995; Eghbali et al., 1991). Furthermore, fibrosis impaired the electrical coupling of cardiomyocytes and reduced cardiac capillary density (Sabbah et al., 1995; Swynghedauw, 1999). Thus, cardiac fibrosis plays key roles in the process of cardiac remodeling.

Piperine is a phenolic component of black pepper and long pepper (Srinivasan, 2007). Previous studies have shown that piperine possesses a number of pharmacological activities. Pharmaceutically, piperine has been reported to protect against hepatotoxicity (Piyachaturawat et al., 1995), attenuate depressive disorders (Bhutani et al., 2009), and mitigate obesity and diabetes (Nogara et al., 2016). It is noteworthy that the administration of piperine and its derivatives resulted in the activation of

Abbreviations: AB, (aortic banding); AKT, (protein kinase B),; AMPKα, (AMP-activated protein kinase α),; ANP, (atrial natriuretic peptide),; BW, (body weight),; BNP, (brain natriuretic peptide),; CF, (cardiac fibroblast),; ERK, (extracellular signal-regulated kinase),; FS, (fractional shortening),; GAPDH, (glyceraldehyde 3-phosphate dehydrogenase),; GSK3β, (glycogen synthase kinase 3β),; HW, (heart weight),; ISO, (isoprenaline),; LVIDd, (left ventricle end-diastolic internal diameter),; MAPK, (mitogen-activated protein kinases),; β-MHC, (β-myosin heavy chain),; PE, (phenylephrine),; PI3K, (phosphatidylinositol-3-kinase),; PPAR-γ, (peroxisome proliferator activated receptor-γ),; α-SMA, (α-smooth muscle actin),; TGF-β, (transforming growth factor-β),; TL, (tibial length).

* Corresponding author at: Department of Cardiology, Renmin Hospital of Wuhan University, Jiefang Road 238, Wuhan 430060, PR China.
E-mail address: qztang@whu.edu.cn (Q.-Z. Tang).

[1] These authors contributed equally to this work.

http://dx.doi.org/10.1016/j.ebiom.2017.03.021

AMPKα signaling in mice (Choi et al., 2013; Kim et al., 2011). Piperine also decreased the phosphorylation of extracellular signal-regulated kinase (ERK) in vitro (Hwang et al., 2011). These findings raised the possibility that piperine could protect against cardiac hypertrophy.

In the current study, we found that piperine-treated mice had similar hypertrophic responses as those treated with the vehicle but developed limited cardiac fibrosis after long-term pressure overload or repeated isoprenaline (ISO) injection independent of the AMPK and MAPK pathway. We also demonstrated that piperine acted as an agonist of peroxisome proliferator that activated receptor-γ (PPAR-γ) and blocked the activation of protein kinase B (AKT).

2. Materials and Methods

2.1. Reagents

Piperine (≥97% purity, as determined by high-performance liquid chromatography) was obtained from Sigma-Aldrich (St. Louis, MO, USA). Isoprenaline (ISO, I5627), TGF-β (T7039), angiotensin II (Ang II, A9525) and phenylephrine (PE, P6126) were purchased from Sigma-Aldrich. The primary antibodies against the following proteins were purchased from Cell Signaling Technology: T-AKT (4691, 1:1000), phospho-AKT (P-AKT, 4060, 1:1000), T-glycogen synthase kinase 3β (GSK3β, 9315, 1:1000), P-GSK3β (9323P, 1:1000), T-P38 (9212P, 1:1000), P-P38 (4511P, 1:1000), T-AMPKα (2603P, 1:1000), P-AMPKα (2535, 1:1000), T-ERK (4695, 1:1000), P-ERK (4370P, 1:1000), T-SMAD3 (3103S, 1:500), P-SMAD3 (3101, 1:500) and glyceraldehyde 3-phosphate dehydrogenase (GAPDH, 2118, 1:1000). α-Smooth muscle actin (α-SMA, ab7817, 1:500) was obtained from Abcam (Cambridge, UK). Antibodies against α-actinin (ab90776) were obtained from Merck Millipore (Massachusetts, United States), and anti-vimentin (sc-5565) was purchased from Santa Cruz Biotechnology (Dallas, TX, USA). The anti-rabbit/mouse EnVisionTM+/HRP reagent used for immunohistochemistry was purchased from Gene Technology (Shanghai, China), and Alexa Fluor 488-goat anti-mouse secondary antibody was purchased from LI-COR Biosciences (Lincoln, USA). The BCA protein assay kit was from Pierce (Rockford, IL, USA).

2.2. Animals and Treatments

All the animal experimental procedures were carried out under the guidance of the Animal Care and Use Committee of Renmin Hospital of Wuhan University, which is also in agreement with the Guidelines for the Care and Use of Laboratory Animals published by the United States National Institutes of Health (NIH Publication, revised 2011). All the animal experimental procedures, including surgery and subsequent analyses, were performed without knowledge of the treatments. C57/B6 mice (male, age: 8–10 weeks; body weight: 25.5 ± 2 g), purchased from the Institute of Laboratory Animal Science, Chinese Academy of Medical Sciences (Beijing, China), were anaesthetized with 3% pentobarbital sodium (50 mg/kg, Sigma) by an intraperitoneal injection. Then, the mice were subjected to aortic banding (AB) or sham surgery as described previously (Jiang et al., 2014). Briefly, the left hemithorax of mouse was shaved, the left chest was opened by performing a ministernotomy, and the thoracic aorta was identified at the second intercostal space. Subsequently, the thoracic aorta was ligated with a 27-G needle using a 7-0 silk suture. Subsequently, the needle was removed, and the thoracic cavity was closed. During the surgery, a heating pad was used to keep the mouse warm. Temgesic (qd, 0.1 mg/kg) was used to relieve postoperative pain. The adequacy of constriction was confirmed via Doppler analysis without knowledge of the treatment. Beginning one week after surgery, the mice were orally treated for 3 weeks with piperine (50 mg/kg diluted in 0.1% DMSO) or vehicle. The dose of piperine was determined according to a previous article (Choi et al., 2013). The chemical structure of piperine has been reported previously (Taqvi et al., 2008). Four weeks after surgery, the mice were sacrificed with an overdose of sodium pentobarbital (200 mg/kg; i.p.) to harvest the hearts. To determine the effect of piperine on agonist-induced cardiac remodeling, we exposed the mice to continuous injection of ISO (50 mg/kg dissolved in sterile saline) for 14 days according to our previous study (Ma et al., 2016a,b).

2.3. Echocardiography and Hemodynamics

Transthoracic echocardiography was performed according to our previous studies (Ma et al., 2016a,b; Wei et al., 2016). Briefly, the mice were anaesthetized by 1.5% isoflurane, and then the left hemithorax was shaved and covered with the pre-warmed ultrasound gel. Transthoracic echocardiography was performed by a MyLab 30CV ultrasound (Esaote SpA, Genoa, Italy) with a 10-MHz linear array ultrasound transducer to obtain M-mode images at the papillary muscle level for measurement of wall thickness, chamber dimensions and cardiac function.

Invasive hemodynamic monitoring was performed to evaluate hemodynamics by cardiac catheterization, which was connected to a Millar Pressure-Volume System (MPVS-400; Millar Instruments). In brief, the mice were anaesthetized with 1.5% isoflurane and ventilated. Then, a 1.4-French Millar catheter transducer (SPR-839; Millar Instruments, Houston, TX) was placed into the left ventricle through the isolated carotid artery for the measurement of left intraventricular pressure. The obtained data were analyzed using PVAN data analysis software.

2.4. Morphometric Analyses and Immunohistochemistry

Hearts obtained from euthanized mice were arrested in diastole and then fixed with 4% formaldehyde overnight. The hearts were embedded in paraffin, sectioned into 5-μm slices, and stained with hematoxylin and eosin (H&E) to count the cardiomyocyte area, and further stained with picrosirius red (PSR) to measure cardiac fibrosis. The cross-sectional area and average collagen volume were counted using a digital analysis system (Image-Pro Plus 6.0, Media Cybernetics, Bethesda, MD, USA). For the detection of the cardiomyocyte area, 50 cells per slide were analyzed. For the determination of fibrosis, >60 fields per group were assessed.

To further evaluate cardiac fibrosis, we performed immunohistochemical staining for α-SMA. Briefly, the paraffin-embedded sections were incubated with anti-α-SMA (ab7817, Abcam, 1:100) overnight at 4 °C and EnVisionTM+/HRP reagent at 37 °C for 30 min. Then, the sections were visualized with diaminobenzidine (DAB) for 2 min at room temperature and mounted with neutral gums. Sections were assessed by light microscopy (Nikon H550L, Tokyo, Japan) and were examined in a blinded fashion by two authors.

2.5. Adenoviral Vectors and Injection

The constitutively active AKT1 and GFP adenoviral (Ad) vectors used in our study were generated by Hanbio Biotechnology Co. (Shanghai, China). To overexpress activated AKT1, mice were given an intramyocardial injection of 1×10^9 viral genome particles (Ad-*Akt* or Ad-*Gfp*, diluted in 15 μL PBS) in 3 locations of the left ventricle (Ma et al., 2016a,b). One week after adenoviral injection, these mice were subjected to injection of ISO for 14 days.

2.6. Western Blot and Quantitative Real-Time PCR

Protein extraction, SDS-PAGE, and immunodetection were performed according to previous articles (Ma et al., 2016a,b; Wei et al., 2016). Protein expression levels were normalized to the matched total proteins or GAPDH. Total mRNA was extracted from tissues or cells with TRIzol reagent (Invitrogen, Carlsbad, CA, USA). Reverse transcription and Real-time PCR were performed as described previously (Ma et al., 2016a,b; Wei et al., 2016). GAPDH was used as an internal control. The primers used are described in Table S1.

2.7. Cell Culture and Treatment

Neonatal rat CFs and neonatal rat cardiac myocytes were isolated according to the previous literature (Aoyama et al., 2005; Sadoshima and Izumo, 1993). CFs and myocytes were seeded at 1×10^6 cells per well in 6-well plates. The myocytes were cultured in DMEM/F12 (GIBCO, C11995) containing 15% FBS (GIBCO, 10099). Bromodeoxyuridine (100 μM) was used to prevent fibroblasts growth in neonatal rat cardiac myocytes. After 16 h of serum starvation, cardiac myocytes were treated with piperine (20 μM, dissolved in 0.1% DMSO) or vehicle followed by PE (50 μM) for 24 h. Cardiomyocytes hypertrophy was evaluated by cell area detected by anti-actinin staining. The cardiac fibroblasts were cultured in DMEM/F12 with 10% FBS. Purity of neonatal CFs was determined by morphologic recognition and by both positive (anti-vimentin) and negative (anti-actinin) staining. Only CFs prior to the third passage were used in our study. After 16 h of serum starvation, CFs were incubated with piperine or vehicle followed by TGF-β1 (10 ng/ml) or Ang II (1 μM) for 24 h. To evaluate the effect of piperine on the proliferative capacity of neonatal CFs, neonatal CFs were incubated with 0% FBS or 10% FBS with or without piperine treatment for different lengths of time. At each point, the cell number was counted using C10227 Countess® automated cell counter (Invitrogen).

Mouse adult CFs were prepared as described previously (Ieda et al., 2009). Briefly, left ventricles from 8-week-old mice were minced and digested in 0.125% trypsin and collagenase at 37 °C. The adult CFs were then suspended in DMEM/F12 medium containing 10% FBS and cultured for 90 min. The attached CFs were cultured for 72 h and used at passages 3–4. After 16 h of serum starvation, adult CFs were treated with piperine and TGF-β1 (10 ng/ml) for 24 h. To assess *Ppar-γ* transactivation, mouse adult CFs were electrotransfected with *Ppre-luc* (0.03 μg) and *Ppar-γ* plasmid (0.3 μg) using Neon® Transfection System (pulse voltage: 1700 V, pulse width: 20 ms). To inhibit PPAR-γ, mouse adult CFs were subjected to a specific PPAR-γ antagonist (GW9662, 10 μM) for 24 h.

For cell transfection, replication-defective adenoviral vectors were used to overexpress constitutively active AKT. Briefly, at 48 h after plating, CFs were infected with adenovirus diluted in DMEM/F12 at 100 MOI. After infection, CFs were starved with FBS-free medium for 16 h and treated with TGF-β1 (10 ng/ml) for 24 h.

2.8. Human Cardiac Fibroblasts Isolation and Culture

All human cardiac tissues were obtained for research purposes in agreement with the Declaration of Helsinki and were also approved by the Renmin Hospital of Wuhan University Review Board. All the hearts ($n = 7$) were obtained from donors (Average age: 48 ± 10 years; EF: 65.6 ± 3.9%) who died accidently but whose hearts could not be transplanted for non-cardiac reasons. The source of these donors has been previously described (Ji et al., 2016). All the families of the donors were aware of the purpose of this study and gave their written informed consent. Human CFs were isolated from left ventricles according to previous studies (Kawano et al., 2000; Neuss et al., 1996). Briefly, the samples were cut into pieces, and digested in 0.125% trypsin and collagenase in a shaking water bath at 37 °C. After digestion, the human CFs were cultured in DMEM/F12 medium containing 10% FBS for 90 min to separate cardiomyocytes. To overexpress constitutively active AKT, human CFs were infected with adenovirus diluted in DMEM/F12 at 100 MOI for 4 h. si*GSK3β* and Silencer® Negative Control #2 siRNA were obtained from Invitrogen. *GSK3β* knockdown was achieved by si*GSK3β* transfection using Lipofectamine RNAiMAX (Invitrogen) for 24 h. The efficiency was confirmed by western blot.

2.9. Immunofluorescence Staining

Cardiac myocytes or CFs were fixed in 4% paraformaldehyde for 15 min and permeabilized in 0.2% Triton X-100 for 10 min. Cardiomyocyte hypertrophy was evaluated using anti-actinin staining. Cardiac myocytes on the glass coverslips were stained with mouse antibody against α-actinin (1:100) and Alexa568-conjugated goat-anti mouse (1:200). CFs on the glass coverslips were stained with mouse antibody against α-SMA (1:100) and Alexa568-conjugated goat-anti mouse (1:200). To visualize nuclei, the slides were mounted with DAPI. Immunofluorescence images were taken on the OLYMPUS DX51 fluorescence microscope (Tokyo, Japan). Images were quantified using Image-Pro Plus 6.0.

2.10. Statistical Analysis

Data in our study are presented as the mean ± standard error of the mean (SEM), and one-way ANOVA was carried out to compare differences among three or more groups followed by post hoc Tukey test. Comparison between two groups was performed using an unpaired Student's *t*-test. A repeated measures ANOVA was also used to compare proliferation capacity of CFs. $P < 0.05$ was considered to be significant.

3. Results

3.1. Piperine Improved Cardiac Function After Chronic Pressure Overload in Mice

Piperine has been reported to decrease body weight and blood pressure in mice (Choi et al., 2013; Taqvi et al., 2008). To exclude the possibility that the protection of piperine was a secondary result, we analyzed the alteration of body weight (BW) and maximum systolic pressure in mice. Compared with mice without piperine protection, mice with piperine treatment exhibited no difference in BW or maximum systolic pressure neither at baseline nor after AB surgery (Fig. 1a–b). No difference in heart rate was observed among the groups (Fig. 1c). After long-term pressure overload, cross-sectional area was increased in mice with pressure overload (Fig. 1a–b). Consistent with the increase in cross-sectional area, after 4 weeks, mice subjected to AB surgery had increased ratios of heart weight (HW) to BW and HW to tibial length (TL) (Fig. 1c–d). Unexpectedly, no difference was found in the extent of hypertrophy between mice with AB + piperine and mice without piperine treatment, though piperine could attenuate the upregulation of atrial natriuretic peptide (ANP) and brain natriuretic peptide (BNP) induced by AB surgery without affecting the mRNA level of β-myosin heavy chain (β-MHC) (Fig. 1a–e). Four weeks after AB surgery, mice without piperine treatment showed a decline in heart function, with a dilated left ventricular diameter and reduced fractional shortening. Conversely, mice with piperine displayed much less AB-induced cardiac dysfunction, with a 10.2% reduction in left ventricle end-diastolic internal diameter (LVIDd) and an 18.5% improvement in fractional shortening (FS) (Fig. 1f). However, there were no significant differences in interventricular septal thickness between AB + vehicle and AB + piperine (Fig. 1d–e). As shown in the pressure-volume analysis, piperine could improve systolic function (assessed by +dP/dt) and diastolic function (as assessed by −dP/dt) after AB surgery (Fig. 1g). Generally, our data demonstrated that piperine could improve cardiac function after pressure overload without affecting the hypertrophic response.

3.2. Piperine Attenuated Cardiac Fibrosis In Vivo

As shown in Fig. 2a–b, compared with mice without piperine treatment, mice with piperine presented a significant decrease in average collagen volume after AB surgery. To further confirm this finding, we detected the expression of α-SMA, a marker of transformation from fibroblasts to myofibroblasts and a landmark in fibrotic remodeling (Dobaczewski et al., 2011). Consistent with the limited collagen volume, we also observed a significant decrease in the intensity of α-SMA in the hearts of mice with piperine (Fig. 2c). The transcript levels of *Tgf-β*, *Collagen I* and *Collagen III* were dramatically increased in the AB-operated

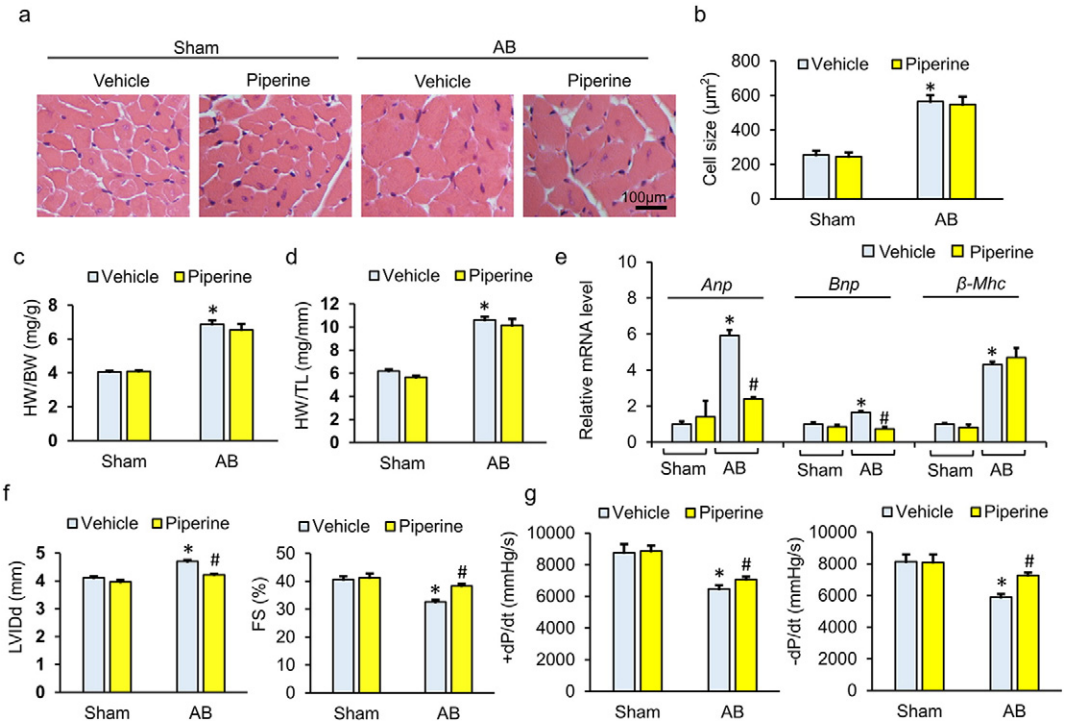

Fig. 1. Piperine improved cardiac function after chronic pressure overload. (a–b) HE staining and the statistical results of cross-sectional area (n = 6). (c–d) Statistical results of the heart weight (HW)/body weight (BW) and HW/tibia length (TL) (n = 12–14). (e) The mRNA levels of hypertrophy-related genes (n = 6). (f) The left ventricular internal diastolic diameter (LVIDd) and fraction shortening (FS) mice from after surgery (n = 8). (g) Hemodynamic analysis of mice with or without piperine treatment (n = 10). Values represent the mean ± SEM. $^{*}P < 0.05$ versus Sham + vehicle, $^{\#}P < 0.05$ versus AB + vehicle.

mice compared with sham-operated mice. Though piperine-treated mice did not exhibit a reduction in the expression of fibrotic genes under basal conditions, treatment with piperine significantly attenuated the AB-induced upregulation of fibrotic markers (Fig. 2d). To further confirm the anti-fibrotic effect of piperine, mice were subjected to repeated injections of ISO to induce cardiac fibrosis. The results showed that piperine-treated mice had a limited fibrotic response, as determined by a decreased average collagen volume and reduced fibrosis-related genes (Fig. 2e–g). Mice with ISO injection also developed cardiac hypertrophy; however, piperine could not block the hypertrophic response induced by ISO (Fig. 2h–i). In view of the fact that low-grade inflammation contributes to the process of cardiac fibrosis, we detected whether piperine attenuated AB caused inflammation and found that the mRNA level of monocyte chemoattractant protein-1 (*Mcp-1*) was slightly downregulated under piperine treatment, whereas tumor necrosis factor-α (*Tnf-α*), interleukin-1β (*Il-1β*) and *Il-6* were unaffected (Fig. 2a–d).

3.3. Piperine Suppressed the Activation of AKT/GSK3β In Vivo

Previous studies demonstrated that piperine suppresses the activation of ERK and activates AMPKα (Choi et al., 2013; Hwang et al., 2011; Kim et al., 2011). Therefore, we checked whether MAPK and AMPKα were responsible for the anti-fibrotic effects of piperine. Contrary to our expectation, piperine did not affect the phosphorylation of AMPKα, P38 and ERK (Fig. 3a–b). TGF-β was the most potent inducer of cardiac fibrosis and promoted the transformation from fibroblast to myofibroblast by activating SMAD3. Having observed that piperine reduced the mRNA level of *Tgf-β*, we next detected the phosphorylation of SMAD3 after piperine treatment and found that pressure overload-induced phosphorylation of SMAD3 was not downregulated in piperine-treated mice (Fig. 3a–b). TGF-β also activated SMAD-independent pathways, including the AKT pathway (Derynck and Zhang, 2003). The activation of AKT and the downstream GSK3β, which is known to be profibrotic, was suppressed in mice treated with piperine (Fig. 3a–b).

3.4. Piperine Inhibited Myofibroblast Transformation Via the AKT/GSK3β Pathway In Vitro

To further explore the protective effects of piperine, neonatal rat cardiac myocytes and fibroblasts were separated. Phenylephrine (PE) was used to induce cardiomyocyte hypertrophy. As expected, PE stimulation resulted in the activation of AKT/GSK3β, and piperine (20 μM) did not affect phosphorylation of AKT/GSK3β in neonatal rat cardiac myocytes (Fig. 3a–b). In line with this finding, cardiomyocytes treated with PE + piperine had a similar cell area compared with cardiomyocytes with PE alone (Fig. 3c). Next, we assessed the effect of piperine on the proliferative capacity of neonatal rat CFs. Piperine-treated neonatal rat CFs had a similar proliferative capacity compared with untreated CFs (Fig. 4a–b). In view of the upregulation of TGF-β in cardiac tissues caused by pressure overload (Fig. 2d), we used TGF-β (10 ng/ml) to stimulate neonatal rat CFs for 24 h. Piperine treatment blocked the TGF-β-mediated increase of collagen synthesis in a dose-dependent manner in neonatal rat CFs (Fig. 4a). We next determined whether piperine had an effect on the transformation of neonatal rat CFs into myofibroblasts by using α-SMA immunostaining. Stimulation of neonatal rat fibroblasts with TGF-β led to a marked increase in expression of α-SMA, and this pathological change was attenuated when neonatal rat CFs were treated with piperine (20 μM), indicating that piperine blocked fibroblasts differentiation into myofibroblasts (Fig. 4b). In agreement with these results, we found that piperine (20 μM) significantly blocked the activation of AKT/GSK3β in neonatal rat CFs (Fig. 4c). To further confirm antifibrotic effects of piperine in vitro, we also used Ang II, another potent inducer of cardiac fibrosis (Crabos et al., 1994). As expected, piperine (20 μM) reduced Ang II-induced phosphorylation of AKT/GSK3β in neonatal rat CFs and prevented the

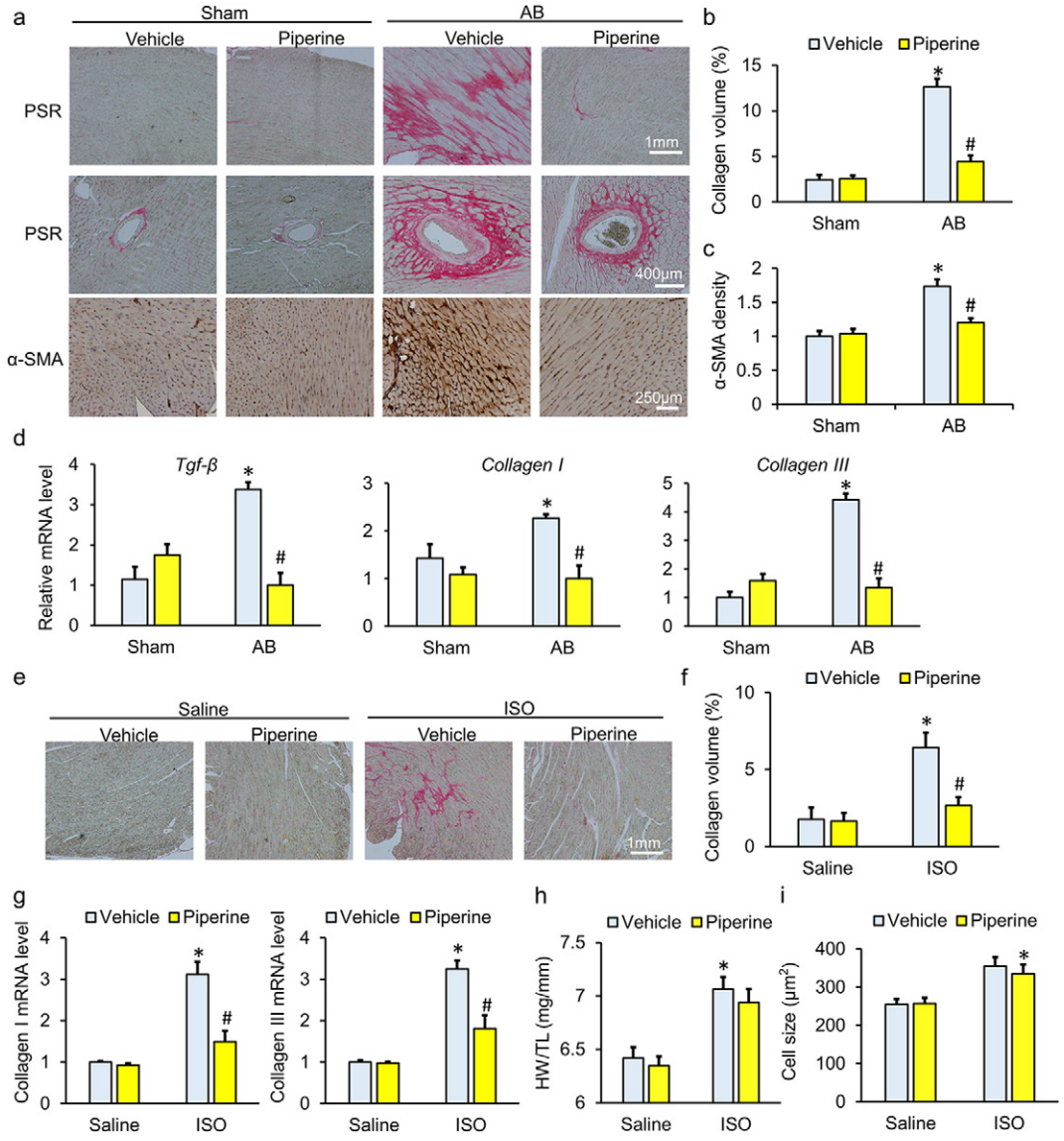

Fig. 2. Piperine attenuated cardiac fibrosis induced by aortic banding (AB) or repeated isoprenaline (ISO) injection. (a) Characteristic images of PSR staining and α-smooth muscle actin (α-SMA) immunostaining. (b) Comparison of the average collagen volume (n = 6). (c) Statistical results of α-SMA immunostaining (n = 6). (d) The mRNA levels of fibrosis-related genes (n = 6). (e–f) PSR staining and the average collagen volume in mice subjected to ISO injection (n = 6). (g) The mRNA levels of fibrosis-related genes (n = 6). (h) Statistical results of the heart weight (HW)/tibia length (TL) (n = 9–10). (i) Results for cross-sectional area (n = 6). Values represent the mean ± SEM. $^{*}P < 0.05$ versus Sham + vehicle, $^{\#}P < 0.05$ versus AB + vehicle.

upregulation of α-SMA expression (Fig. 5a–d). To verify the hypothesis that AKT was involved in the antifibrotic effects of piperine, neonatal rat CFs were subjected to adenoviral infection to overexpress constitutively active AKT (Fig. 6a). Of note, piperine lost its protective effect in the presence of overexpressed, constitutively active AKT, as indicated by mRNA levels of *Collagen 1* and *Collagen III* (Fig. 4d). Considering that neonatal CFs differ in phenotypic plasticity from adult CFs, mouse adult CFs were used. Consistent with the findings in neonatal CFs, piperine had no effect on the transformation of adult mouse CFs into myofibroblasts after adenoviral infection (Fig. 4e, 6b). To enhance the clinical impact of our current work, we isolated human ventricle CFs. Piperine treatment also reduced the production of α-SMA, and this effect was lost after constitutively active AKT overexpression in human adult CFs (Fig. 4f). Next, we tested the hypothesis that reduced phosphorylation of GSK3β by piperine is required for the antifibrotic effects of piperine in human CFs. We incubated human CFs with si*GSK3β* and found that the effects of piperine were blocked after the knockdown of *GSK3β* (Fig. 7a–b).

3.5. Piperine Had no Protective Effects on Cardiac Fibrosis in Mice With Constitutively Active AKT

To further investigate whether piperine exerted antifibrotic effects through AKT/GSK3β in vivo, mice were infected with adenoviral vectors carrying constitutively active AKT. Overexpression of constitutively active AKT did not affect the hypertrophic response induced by ISO injection (Fig. 8a–d). Chronic ISO injection increased average collagen volume, α-SMA intensity and collagen accumulation, which was attenuated by piperine treatment in mice infected with Ad-*Gfp* but not in mice infected with Ad-*Akt* (Fig. 5a–f).

3.6. Piperine Reduced Phosphorylation of AKT Via Activating PPAR-γ Receptor

Previous study has reported that piperine could function as a PPAR-γ agonist (Kharbanda et al., 2016). We previously found that pioglitazone (PIO), another PPAR-γ agonist, attenuated pressure overload-induced

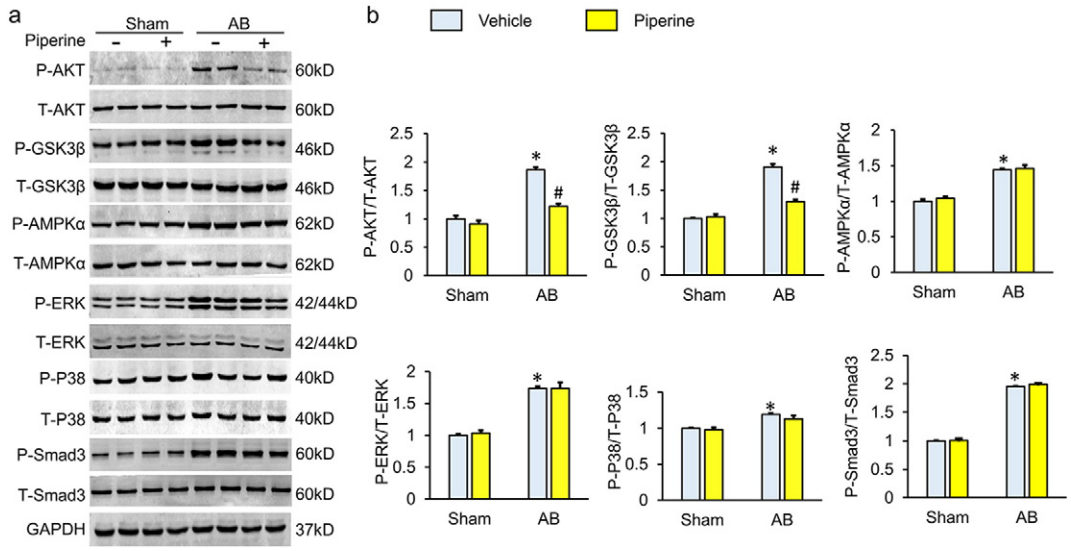

Fig. 3. Piperine inhibited the activation of the AKT/GSK3β pathway. (a–b) Representative western blots and quantitative results (n = 6). Values represent the mean ± SEM. $^{*}P < 0.05$ versus Sham + vehicle, $^{\#}P < 0.05$ versus AB + vehicle.

cardiac hypertrophy and fibrosis via the attenuation of AKT/GSK3β (Wei et al., 2016). We hypothesized that piperine inhibited cardiac fibrosis via activating PPAR-γ. First, we compared piperine with pioglitazone in *Ppar-γ* transactivation. Pioglitazone strongly transactivated *Ppar-γ* in mouse adult CFs, whereas piperine (20 μM) was found to activate *Ppar-γ* comparatively to a lesser extent (Fig. 6a). Piperine (20 μM) exhibited a 2.5-fold increase in *Ppar-γ* gene expression in mouse adult CFs, which has been shown to be less effective than pioglitazone (Fig. 6b). Intriguingly, GW9662 (an irreversible PPAR-γ antagonist), which alone did not affect the expression of *α-Sma* (Fig. 6c–d), completely blocked the protective effects of piperine on fibroblasts transformation and AKT/GSK3β in mouse adult CFs (Fig. 6c–d).

4. Discussion

Here, for the first time, we demonstrated that piperine protected against cardiac fibrosis induced by pressure overload or repeated ISO injection in vivo. Piperine blocked the transformation of fibroblasts to myofibroblasts induced by TGF-β or Ang II in vitro. The protection of piperine was mediated by the attenuation of the AKT/GSK3β pathway. Constitutively active AKT overexpression or GSK3β knockdown in CFs could abolish piperine-mediated protection. We also found that piperine activated PPAR-γ receptors in CFs.

It has been reported that piperine could activate AMPK signaling and reduce the phosphorylation of ERK (Choi et al., 2013; Hwang et al., 2011; Kim et al., 2011). In view of our previous studies on drugs activating AMPK and inhibiting ERK to protect against pressure overload-induced cardiac hypertrophy (Ma et al., 2016a,b), we hypothesized that piperine could be an effective therapeutic candidate against cardiac hypertrophy. Beyond our expectations, piperine treatment did not affect hypertrophic response but significantly blocked the fibrotic response induced by AB surgery or ISO administration. In line with this finding, we found that piperine inhibited ventricular dilatation and improved cardiac function without affecting interventricular septal thickness, implying that piperine prevented cardiac dilation but not ventricular hypertrophy. Cardiac fibrosis resulted in adverse mechanical and electrical disturbances in diseased hearts, promoting the progression of HF (Sabbah et al., 1995). Drugs with demonstrable efficacy in trials have not exhibited similar effectiveness in clinical practice. Our findings provided an opportunity to bridge this gap.

AKT/GSK3β pathway plays a critical role in the pathological fibrotic response. TGF-β increased the phosphorylation of AKT by activating phosphatidylinositol-3-kinase (PI3K) (Derynck and Zhang, 2003). The inhibition of AKT significantly attenuates cardiac fibrosis induced by pressure overload (Wei et al., 2016). Activated AKT directly phosphorylates and inactivated GSK3β, which regulates the general protein translational machinery (Hardt and Sadoshima, 2002). The fibroblast-specific deletion of *Gsk3β* increases the post-myocardial infarction scar circumference and fibrosis (Lal et al., 2014). Here, we found that piperine reduced the phosphorylation of AKT and GSK3β in vivo and in vitro. The overexpression of constitutively active AKT or the knockdown of *GSK3β* offset the protective effects of piperine in CFs. Our studies suggest that the attenuation of AKT/GSK3β signaling following piperine treatment is the primary mechanism leading to a limited fibrotic response.

To date, cell- and rodent-based studies have advanced our understanding of how PPAR-γ regulates cardiac fibrosis. Mice with defective *Ppar-γ* develop a more severe cardiac fibrotic response to Ang II (Kis et al., 2009). The pharmacological activation and overexpression of PPAR-γ blocks TGF-β-induced collagen accumulation in CFs (Gong et al., 2011). In line with these observations, we previously found that pioglitazone reduces activated MAPK pathways and AKT/GSK3β, thereby suppressing cardiac fibrosis induced by pressure overload (Wei et al., 2016). Piperine exerts its protection as an agonist of PPAR-γ. In docking studies, piperine had a higher dock score than did rosiglitazone (Kharbanda et al., 2016). In agreement with this finding, we found that piperine transactivated PPAR-γ and increased the mRNA level of *Ppar-γ*. Importantly, our in vitro experiments demonstrated that piperine loses its protective function against myoblast transformation in cells pretreated with GW9662, further supporting our hypothesis that piperine exerted protective effects by activating PPAR-γ.

Intriguingly, although activating PPAR-γ resulted in the attenuation of the AKT pathway, the underlying mechanisms mediating the PPAR-γ agonist-induced suppression of AKT were discordant. Wei et al. found that a synthetic oleanane triterpenoid activated PPAR-γ and inhibited AKT signaling independent of PPAR-γ (Wei et al., 2014). Kulkarni et al. found that the electrophilic center present in PPAR-γ ligands is of great importance to their ability to suppress phosphorylation of AKT (Kulkarni et al., 2011). Inconsistent with these aforementioned studies, the data in our study suggested that piperine reduced the phosphorylation of AKT dependent of PPAR-γ, in line with the finding that PPAR-γ could bind the *Pten* promoter and upregulate PTEN expression, thus suppressing the AKT pathway (Patel et al., 2001).

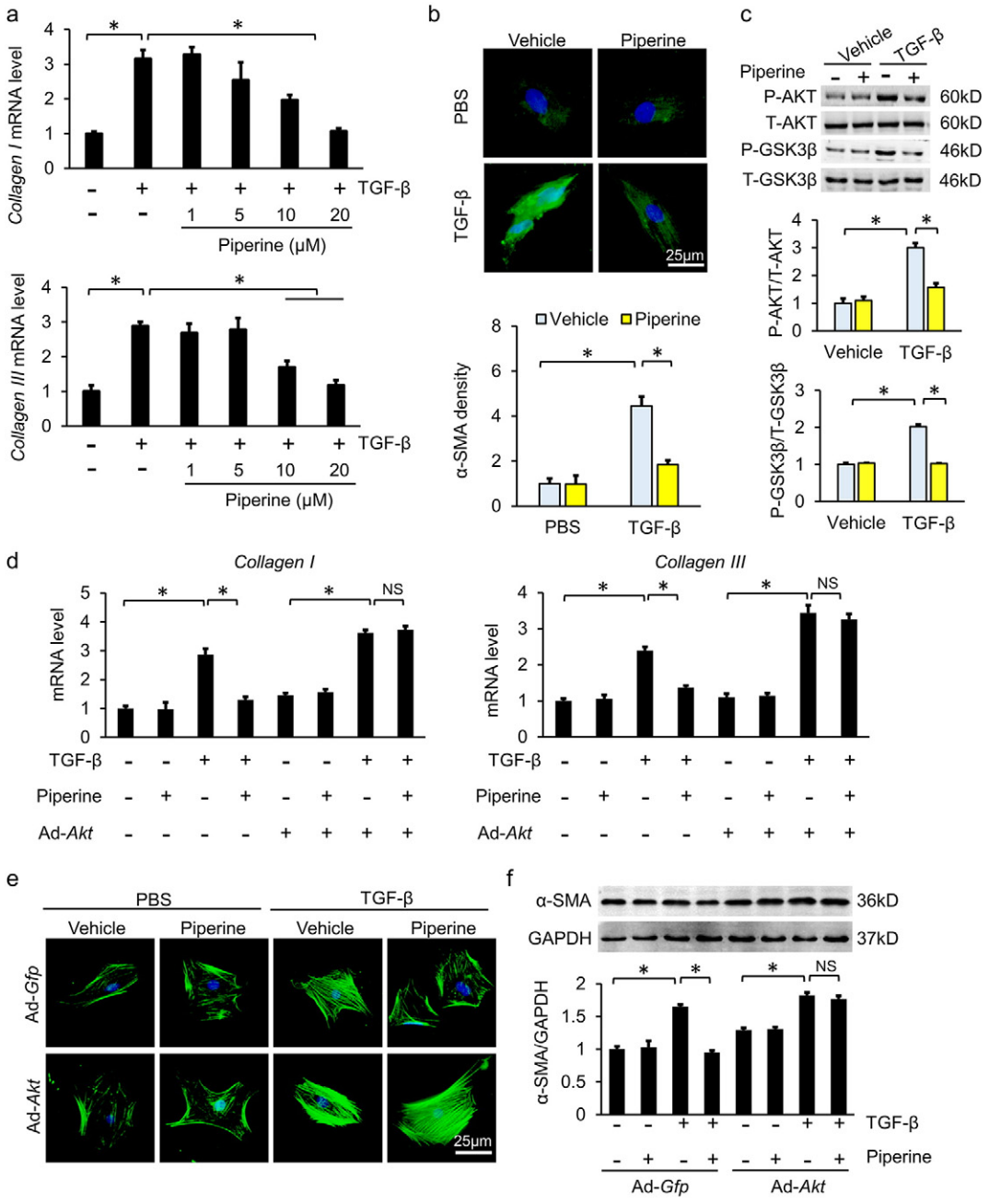

Fig. 4. Piperine blocked the transformation of cardiac fibroblasts (CFs) to myofibroblasts induced by transforming growth factor-β (TGF-β). (a) Comparison of mRNA levels of *Collagen I* and *Collagen III* in neonatal rat CFs (n = 6). (b) Representative images of α-smooth muscle actin (α-SMA, green)-stained neonatal rat CFs and statistical results (n = 6). Nuclei were stained with DAPI (blue). (c) Alteration of the AKT/GSK3β pathway in neonatal rat CFs after piperine treatment (n = 6). (d) The mRNA levels of *Collagen I* and *Collagen III* in neonatal rat CFs infected with adenovirus carrying constitutively active AKT (n = 6). (e) Representative images of α-SMA-stained mouse adult CFs after infection with constitutively active AKT adenovirus (n = 6). Nuclei were stained with DAPI (blue). (f) The α-SMA protein expression in human adult CFs after infection for the expression of constitutively active AKT (n = 6). Values represent the mean ± SEM. $^{*}P < 0.05$ versus the matched control. NS; no significance.

Agonists of PPAR-γ, including rosiglitazone and pioglitazone, have been used for treating metabolic disorders. Due to increased cardiovascular risks, their therapeutic use is limited. The side effects of thiazolidinedione are largely attributed to its high affinity for PPAR-γ and overactivation of the PPAR-γ pathway (Larsen et al., 2008; Nesto et al., 2004). In our study, compared with pioglitazone, piperine could moderately transactivate PPAR-γ, implying that piperine may partially activate PPAR-γ. In addition, adverse events, such as increased cardiac risks and weight gain, were not observed in mice with piperine treatment. Taken together, piperine has the potential for development in clinical use.

In conclusion, we found that piperine inhibited cardiac fibrosis via the PPAR-γ-dependent attenuation of the AKT/GSK3β pathway. Our study provides evidence for the application of piperine in the treatment of cardiac fibrosis.

Conflicts of Interest

None.

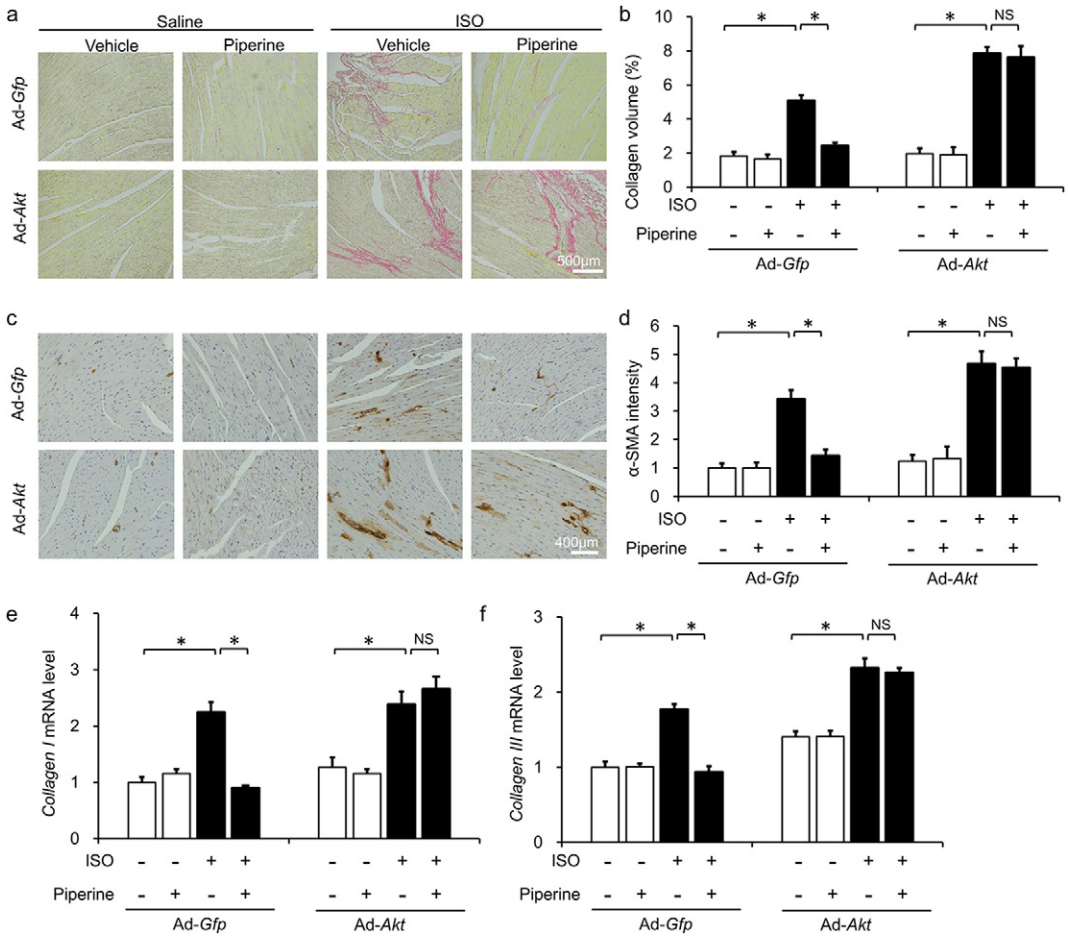

Fig. 5. Infection for the expression of constitutively active AKT blocked the protection of piperine against cardiac fibrosis in vivo (n = 10). (a–b) PSR staining and average collagen volume (n = 6). (c–d) α-Smooth muscle actin (α-SMA) immunostaining and statistical results (n = 6). (e–f) The mRNA levels of *Collagen I* and *Collagen III* (n = 6). Values represent the mean ± SEM. $^{*}P < 0.05$ versus the matched control. NS; no significance.

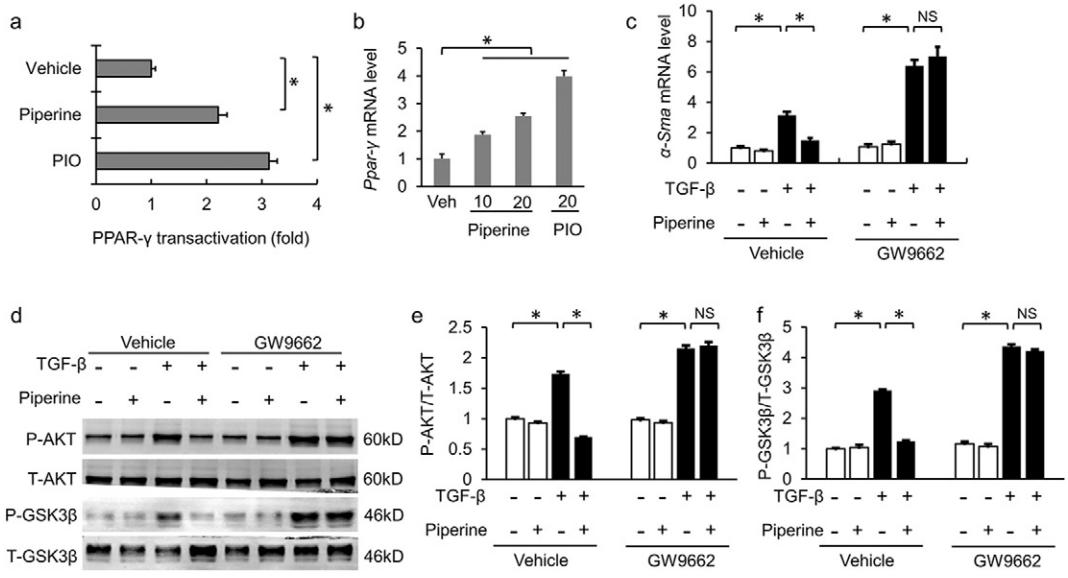

Fig. 6. Piperine acted as an agonist of peroxisome proliferator activated receptor-γ (PPAR-γ). (a) The effect of piperine on *Ppar-γ* transactivation in mouse adult CFs (n = 6). (b) The mRNA level of *Ppar-γ* in mouse adult CFs (n = 6). (c) The mRNA level of *α-Sma* in mouse adult CFs after GW9662 treatment (n = 6). (d–f) Alterations in the AKT/GSK3β pathway after GW9662 treatment in mouse adult CFs (n = 6). Values represent the mean ± SEM. $^{*}P < 0.05$ versus the matched control. NS; no significance. Veh, vehicle; PIO, pioglitazone.

Funding Sources

This work was supported by grants from National Natural Science Foundation of China (No: 81270303, 81470516, 81470402, 81500184), the Key Project of the National Natural Science Foundation of China (No. 81530012), and the Research Program from the Department of Science and Technology of Hunan Province (No. 2015SK20455).

Author Contributions

Z.G.M, Y.P.Y, X.Z, S.C.X and S.S.W performed the study, analyzed the data, and wrote the manuscript. Z.G.M, Y.P.Y, S.C.X, X.Z and Q.Z.T contributed to the acquisition of data and to manuscript preparation and revision. Z.G.M, Y.P.Y and Q.Z.T conceived of the hypothesis and participated in the experimental design, data interpretation, and manuscript preparation and revision. All authors approved the final version of the manuscript.

Acknowledgements

None.

Appendix A. Supplementary data

Supplementary data to this article can be found online at http://dx.doi.org/10.1016/j.ebiom.2017.03.021.

References

Aoyama, T., Matsui, T., Novikov, M., Park, J., Hemmings, B., Rosenzweig, A., 2005. Serum and glucocorticoid-responsive kinase-1 regulates cardiomyocyte survival and hypertrophic response. Circulation 111, 1652–1659.

Bhutani, M.K., Bishnoi, M., Kulkarni, S.K., 2009. Anti-depressant like effect of curcumin and its combination with piperine in unpredictable chronic stress-induced behavioral, biochemical and neurochemical changes. Pharmacol. Biochem. Behav. 92, 39–43.

Butt, R.P., Laurent, G.J., Bishop, J.E., 1995. Collagen production and replication by cardiac fibroblasts is enhanced in response to diverse classes of growth factors. Eur. J. Cell Biol. 68, 330–335.

Chan, A.Y.J., Dyck, R., 2005. Activation of AMP-activated protein kinase (AMPK) inhibits protein synthesis: a potential strategy to prevent the development of cardiac hypertrophy. Can. J. Physiol. Pharmacol. 83, 24–28.

Choi, S., Choi, Y., Choi, Y., Kim, S., Jang, J., Park, T., 2013. Piperine reverses high fat diet-induced hepatic steatosis and insulin resistance in mice. Food Chem. 141, 3627–3635.

Crabos, M., Roth, M., Hahn, A.W., Erne, P., 1994. Characterization of angiotensin II receptors in cultured adult rat cardiac fibroblasts. Coupling to signaling systems and gene expression. J. Clin. Invest. 93, 2372–2378.

Derynck, R., Zhang, Y.E., 2003. Smad-dependent and Smad-independent pathways in TGF-beta family signalling. Nature 425, 577–584.

Dobaczewski, M., Chen, W., Frangogiannis, N.G., 2011. Transforming growth factor (TGF)-beta signaling in cardiac remodeling. J. Mol. Cell. Cardiol. 51, 600–606.

Eghbali, M., Tomek, R., Woods, C., Bhambi, B., 1991. Cardiac fibroblasts are predisposed to convert into myocyte phenotype: specific effect of transforming growth factor beta. Proc. Natl. Acad. Sci. U. S. A. 88, 795–799.

Frey, N.E., Olson, N., 2003. Cardiac hypertrophy: the good, the bad, and the ugly. Annu. Rev. Physiol. 65, 45–79.

Gong, K., Chen, Y.F., Li, P., Lucas, J.A., Hage, F.G., Yang, Q., Nozell, S.E., Oparil, S., Xing, D., 2011. Transforming growth factor-beta inhibits myocardial PPARγ expression in pressure overload-induced cardiac fibrosis and remodeling in mice. J. Hypertens. 29, 1810–1819.

Hardt, S.E., Sadoshima, J., 2002. Glycogen synthase kinase-3beta: a novel regulator of cardiac hypertrophy and development. Circ. Res. 90, 1055–1063.

Heineke, J., Molkentin, J.D., 2006. Regulation of cardiac hypertrophy by intracellular signalling pathways. Nat. Rev. Mol. Cell Biol. 7, 589–600.

Hwang, Y.P., Yun, H.J., Kim, H.G., Han, E.H., Choi, J.H., Chung, Y.C., Jeong, H.G., 2011. Suppression of phorbol-12-myristate-13-acetate-induced tumor cell invasion by piperine via the inhibition of PKCα/ERK1/2-dependent matrix metalloproteinase-9 expression. Toxicol. Lett. 203, 9–19.

Ieda, M., Tsuchihashi, T., Ivey, K.N., Ross, R.S., Hong, T.T., Shaw, R.M., Srivastava, D., 2009. Cardiac fibroblasts regulate myocardial proliferation through beta 1 integrin signaling. Dev. Cell 16, 233–244.

Ji, Y.X., Zhang, P., Zhang, X.J., Zhao, Y.C., Deng, K.Q., Jiang, X., Wang, P.X., Huang, Z., Li, H., 2016. The ubiquitin E3 ligase TRAF6 exacerbates pathological cardiac hypertrophy via TAK1-dependent signalling. Nat. Commun. 7, 11267.

Jiang, D.S., Wei, X., Zhang, X.F., Liu, Y., Zhang, Y., Chen, K., Gao, L., Zhou, H., Zhu, X.H., Liu, P.P., Bond, Lau W., Ma, X., Zou, Y., Zhang, X.D., Fan, G.C., Li, H., 2014. IRF8 suppresses pathological cardiac remodelling by inhibiting calcineurin signalling. Nat. Commun. 5, 3303.

Kamo, T., Akazawa, H., Komuro, I., 2015. Cardiac nonmyocytes in the hub of cardiac hypertrophy. Circ. Res. 117, 89–98.

Kawano, H., Do, Y.S., Kawano, Y., Starnes, V., Barr, M., Law, R.E., Hsueh, W.A., 2000. Angiotensin II has multiple profibrotic effects in human cardiac fibroblasts. Circulation 101, 1130–1137.

Kharbanda, C., Alam, M.S., Hamid, H., Javed, K., Bano, S., Ali, Y., Dhulap, A., Alam, P., Pasha, M.A., 2016. Novel piperine derivatives with antidiabetic effect as PPAR-γ agonists. Chem. Biol. Drug Des. 88, 354–362.

Kim, K.J., Lee, M.S., Jo, K., Hwang, J.K., 2011. Piperidine alkaloids from *Piper retrofractum* Vahl. protect against high-fat diet-induced obesity by regulating lipid metabolism and activating AMP-activated protein kinase. Biochem. Biophys. Res. Commun. 411, 219–225.

Kis, A., Murdoch, C., Zhang, M., Siva, A., Rodriguez-Cuenca, S., Carobbio, S., Lukasik, A., Blount, M., O'Rahilly, S., Gray, S.L., Shah, A.M., Vidal-Puig, A., 2009. Defective peroxisomal proliferators activated receptor gamma activity due to dominant-negative mutation synergizes with hypertension to accelerate cardiac fibrosis in mice. Eur. J. Heart Fail. 11, 533–541.

Kulkarni, A.A., Thatcher, T.H., Olsen, K.C., Maggirwar, S.B., Phipps, R.P., Sime, P.J., 2011. PPAR-γ ligands repress TGFβ-induced myofibroblast differentiation by targeting the PI3K/Akt pathway: implications for therapy of fibrosis. PLoS One 6, e15909.

Lal, H., Ahmad, F., Zhou, J., Yu, J.E., Vagnozzi, R.J., Guo, Y., Yu, D., Tsai, E.J., Woodgett, J., Gao, E., Force, T., 2014. Cardiac fibroblast glycogen synthase kinase-3beta regulates ventricular remodeling and dysfunction in ischemic heart. Circulation 130, 419–430.

Larsen, P.J., Lykkegaard, K., Larsen, L.K., Fleckner, J., Sauerberg, P., Wassermann, K., Wulff, E.M., 2008. Dissociation of antihyperglycaemic and adverse effects of partial perioxisome proliferator-activated receptor (PPAR-gamma) agonist balaglitazone. Eur. J. Pharmacol. 596, 173–179.

Lorenz, K., Schmitt, J.P., Vidal, M., Lohse, M.J., 2009. Cardiac hypertrophy: targeting Raf/MEK/ERK1/2-signaling. Int. J. Biochem. Cell Biol. 41, 2351–2355.

Ma, Z.G., Dai, J., Zhang, W.B., Yuan, Y., Liao, H.H., Zhang, N., Bian, Z.Y., Tang, Q.Z., 2016a. Protection against cardiac hypertrophy by geniposide involves the GLP-1 receptor/AMPKα signalling pathway. Br. J. Pharmacol. 173, 1502–1516.

Ma, Z.G., Dai, J., Wei, W.Y., Zhang, W.B., Xu, S.C., Liao, H.H., Yang, Z., Tang, Q.Z., 2016b. Asiatic acid protects against cardiac hypertrophy through activating AMPKα signalling pathway. Int. J. Biol. Sci. 12, 861–871.

Nesto, R.W., Bell, D., Bonow, R.O., Fonseca, V., Grundy, S.M., Horton, E.S., Le Winter, M., Porte, D., Semenkovich, C.F., Smith, S., Young, L.H., Kahn, R., 2004. Thiazolidinedione use, fluid retention, and congestive heart failure: a consensus statement from the American Heart Association and American Diabetes Association. Diabetes Care 27, 256–263.

Neuss, M., Regitz-Zagrosek, V., Hildebrandt, A., Fleck, E., 1996. Isolation and characterisation of human cardiac fibroblasts from explanted adult hearts. Cell Tissue Res. 286, 145–153.

Nogara, L., Naber, N., Pate, E., Canton, M., Reggiani, C., Cooke, R., 2016. Piperine's mitigation of obesity and diabetes can be explained by its up-regulation of the metabolic rate of resting muscle. Proc. Natl. Acad. Sci. U. S. A. 113, 13009–13014.

Patel, L., Pass, I., Coxon, P., Downes, C.P., Smith, S.A., Macphee, C.H., 2001. Tumor suppressor and anti-inflammatory actions of PPARgamma agonists are mediated via upregulation of PTEN. Curr. Biol. 11, 764–768.

Piyachaturawat, P., Kingkaeohoi, S., Toskulkao, C., 1995. Potentiation of carbon tetrachloride hepatotoxicity by piperine. Drug Chem. Toxicol. 18, 333–344.

Ravingerova, T., Barancik, M., Strniskova, M., 2003. Mitogen-activated protein kinases: a new therapeutic target in cardiac pathology. Mol. Cell. Biochem. 247, 127–138.

Sabbah, H.N., Sharov, V.G., Lesch, M., Goldstein, S., 1995. Progression of heart failure: a role for interstitial fibrosis. Mol. Cell. Biochem. 147, 29–34.

Sadoshima, J., Izumo, S., 1993. Molecular characterization of angiotensin II-induced hypertrophy of cardiac myocytes and hyperplasia of cardiac fibroblasts. Critical role of the AT1 receptor subtype. Circ. Res. 73, 413–423.

Srinivasan, K., 2007. Black pepper and its pungent principle-piperine: a review of diverse physiological effects. Crit. Rev. Food Sci. Nutr. 47, 735–748.

Swynghedauw, B., 1999. Molecular mechanisms of myocardial remodeling. Physiol. Rev. 79, 215–262.

Taqvi, S.I., Shah, A.J., Gilani, A.H., 2008. Blood pressure lowering and vasomodulator effects of piperine. J. Cardiovasc. Pharmacol. 52, 452–458.

Wei, J., Zhu, H., Komura, K., Lord, G., Tomcik, M., Wang, W., Doniparthi, S., Tamaki, Z., Hinchcliff, M., Distler, J.H., Varga, J., 2014. A synthetic PPAR-γ agonist triterpenoid ameliorates experimental fibrosis: PPAR-γ-independent suppression of fibrotic responses. Ann. Rheum. Dis. 73, 446–454.

Wei, W.Y., Ma, Z.G., Xu, S.C., Zhang, N., Tang, Q.Z., 2016. Pioglitazone protected against cardiac hypertrophy via inhibiting AKT/GSK3β and MAPK signaling pathways. PPAR Res. 2016, 9174190.

Zhang, P., Hu, X., Xu, X., Fassett, J., Zhu, G., Viollet, B., Xu, W., Wiczer, B., Bernlohr, D.A., Bache, R.J., Chen, Y., 2008. AMP activated protein kinase-alpha 2 deficiency exacerbates pressure-overload-induced left ventricular hypertrophy and dysfunction in mice. Hypertension 52, 918–924.